

# Endogenous sulfur dioxide protects against isoproterenol-induced myocardial injury and increases myocardial antioxidant capacity in rats

Yinfang Liang<sup>1,\*</sup>, Die Liu<sup>1,\*</sup>, Todd Ochs<sup>2</sup>, Chaoshu Tang<sup>3,4</sup>, Stella Chen<sup>5</sup>, Suqing Zhang<sup>1</sup>, Bin Geng<sup>3,4</sup>, Hongfang Jin<sup>1</sup> and Junbao Du<sup>1,4</sup>

Recently, sulfur dioxide (SO<sub>2</sub>) was discovered to be produced in the cardiovascular system and to influence important biological processes. Here, we investigated changes in endogenous SO<sub>2</sub>/glutamic oxaloacetic transaminase (GOT) pathway in the development of isoproterenol (ISO)-induced myocardial injury in rats and the regulatory effect of SO<sub>2</sub> on cardiac function, myocardial micro- and ultrastructure, and oxidative stress. Wistar male rats were divided into control, ISO-treated, ISO + SO<sub>2</sub>, and SO<sub>2</sub> groups. At the termination of the experiment, parameters of cardiac function and hemodynamics were measured and the micro- and ultrastructure of myocardium and stereological ultrastructure of mitochondria were analyzed. Myocardial SO<sub>2</sub> content was detected by high-performance liquid chromatography. GOT (key enzyme for endogenous SO<sub>2</sub> production) activity and gene (*GOT1* and *GOT2*) expressions were measured, and superoxide dismutase (SOD), glutathione peroxidase (GSH-Px), hydrogen peroxide, and superoxide radical levels were assayed. *SOD* (*SOD1* and *SOD2*) and *GSH-Px* (*GSH-Px1*) gene expressions were also detected. The results showed that SO<sub>2</sub> donor at a dose of 85 mg/(kg day) did not impact the cardiac function and structure of rats, but exerted a subtle influence on myocardial redox status. ISO-treated rats exhibited decreased cardiac function, damaged myocardial structures, and downregulated endogenous SO<sub>2</sub>/GOT pathway. Meanwhile, myocardial oxidative stress increased, whereas antioxidative capacity downregulated. Administration of SO<sub>2</sub> markedly improved cardiac function and ISO-induced myocardial damage by ameliorating the pathological structure of the myocardium and the mitochondria. At the same time, myocardial products of oxidative stress decreased, whereas antioxidative capacity increased. These results suggest that down-regulation of the endogenous SO<sub>2</sub>/GOT pathway is likely involved in the pathogenesis of ISO-induced myocardial injury. SO<sub>2</sub> protects against ISO-induced myocardial injury associated with increased myocardial antioxidant capacity in rats.

*Laboratory Investigation* (2011) 91, 12–23; doi:10.1038/labinvest.2010.156; published online 23 August 2010

**KEYWORDS:** antioxidant capacity; isoproterenol; myocardial injury; sulfur dioxide

Myocardial injury is a common feature in a variety of cardiac diseases. Factors proposed to be involved in its mechanism include hypoxia due to myocardial hyperactivity and coronary hypotension, calcium overload, depletion of energy reserves, and excessive production of oxygen-free radicals, resulting from the oxidative metabolism of catecholamines. The oxidative products of catecholamines affect the cardiac myocyte membrane and depress cardiac contractile activity, which are followed by damages in the mitochondria, the sarcotubular system, and contractile elements.<sup>1</sup> Previous studies have shown

isoproterenol (ISO)-induced cardiotoxicity to be related to the formation of oxygen-free radicals and sulfhydryl reactivity through a variety of oxidative products.<sup>2</sup> Oxygen-free radicals, in turn, may increase membrane permeability by promoting lipid peroxidation, leading to the development of cardiac injury.<sup>3</sup> However, the mechanism responsible for myocardial injury is not completely understood.

Sulfur dioxide (SO<sub>2</sub>) was only considered as a common air pollutant in the past. Long-term exposure to high dose of SO<sub>2</sub> has toxic effects.<sup>4–6</sup> Interestingly, however, sulfur amino

<sup>1</sup>Department of Pediatrics, Peking University First Hospital, Beijing, PR China; <sup>2</sup>Northwestern University, Chicago, IL, USA; <sup>3</sup>Department of Physiology and Pathophysiology, Peking University Health Science Center, Beijing, PR China; <sup>4</sup>Key Laboratory of Molecular Cardiovascular Diseases, Ministry of Education, Beijing, PR China and <sup>5</sup>Department of Biochemistry and Cellular Biology, University of California, San Diego, La Jolla, CA, USA

Correspondence: Professor J Du, MD or Dr H Jin, PhD, Department of Pediatrics, Peking University First Hospital, Beijing 100034, PR China.

E-mail: junbaodu1@126.com or jinhongfang51@126.com

\*These two authors contributed equally to this work.

Received 19 October 2009; revised 13 July 2010; accepted 20 July 2010

acid metabolism in the human body may generate  $\text{SO}_2$ . As reported in literature,  $\text{SO}_2$  could be derived from various types of sulfur amino acid metabolism in the body.<sup>7</sup> The generation of  $\text{SO}_2$  from L-cysteine occurs as follows: cysteine oxidase oxidizes L-cysteine to L-cysteinesulfinate, and the latter, by two competing pathways of decarboxylation and transamination, changes to hypotaurine and  $\beta$ -sulfinylpyruvate, respectively, and is finally metabolized to taurine and pyruvate.<sup>8</sup> Through glutamic oxaloacetic transaminase (GOT), L-cysteinesulfinate is transformed into  $\beta$ -sulfinyl acetone acid ( $\beta$ -sulfinylpyruvate), which spontaneously divides into pyruvate and  $\text{SO}_2$ . *In vivo*,  $\text{SO}_2$  reacts with water, becoming  $\text{SO}_3^{2-}$ , which in turn changes into  $\text{SO}_4^{2-}$  after being catalyzed by sulfite oxidase (Figure 1).

Ji *et al*<sup>9</sup> used high performance liquid chromatography (HPLC) to detect the total serum concentrations of sulfite in normal subjects. Investigators identified  $\text{SO}_2$  in coronary artery, which was suggested to be an endothelium-derived hyperpolarizing factor.<sup>10</sup> Recently, our research group found that  $\text{SO}_2$  could be endogenously generated in vascular tissues, such as aorta, pulmonary artery, mesenteric artery, tail artery and renal artery, and aorta had the highest  $\text{SO}_2$  content among the vascular tissues tested. We also found that aortic aspartate aminotransferase mRNA situated at endothelium and vascular smooth muscle cells near the endothelial layer.<sup>7</sup>

Previously, the biological role of  $\text{SO}_2$  had not been studied thoroughly.<sup>10</sup> Zhang, from our research group,<sup>11</sup> proved that endogenous  $\text{SO}_2$  had an important role in the regulation of myocardial ischemia–reperfusion. Recent studies revealed that exogenous  $\text{SO}_2$  has a role in the inflammatory response.<sup>12–14</sup> Endogenous  $\text{SO}_2$  may be a biologically active molecule involved in the regulation of cardiovascular function, demonstrated by the regulatory role in the myocardial ischemia–reperfusion.<sup>11</sup> The above findings suggested that

endogenous  $\text{SO}_2$  might be an important mediator in the cardiovascular system, but it remains unclear whether and how endogenous  $\text{SO}_2$  contributes to the pathophysiological process of myocardial injury.

To evaluate the role of the  $\text{SO}_2$ /GOT pathway in the pathogenesis of myocardial injury, we attempted to observe the changes in the endogenous myocardial  $\text{SO}_2$ /GOT pathway that occurs during the development of a commonly used experimental rat model of myocardial injury, ISO-induced myocardial injury, and identify the regulatory effect of  $\text{SO}_2$  on the myocardial structure and function, and oxidative stress as well.

## MATERIALS AND METHODS

### Animal Preparation and Reagents

Experimental protocols complied with the Animal Management Guidelines of the Ministry of Health of the People's Republic of China, and the Guide for the Care and Use of Laboratory Animals of Peking University First Hospital (Beijing, PR China).

Male Wistar rats (220–250 g) were provided by the Animal Department, Health Science Center of Peking University. ISO, sodium sulfite/sodium bisulfite ( $\text{Na}_2\text{SO}_3/\text{NaHSO}_3$ , the  $\text{SO}_2$  donor), and monobromobimane (mBrB) were purchased from Sigma (St Louis, MO, USA); Trizol was from Gibco (BRL, Rockville, MD, USA); and deoxyribonucleotide triphosphate (dNTP), Moloney murine leukemia virus reverse transcriptase (MMLV RT), oligo-(dT)<sub>15</sub>, and Taq DNA polymerase were from Promega (Madison, WI, USA). Other chemicals and reagents were of analytical grade.

A total of 46 rats were randomly divided into four groups: control group ( $n=16$ ), ISO-treated group ( $n=12$ ), ISO- $\text{SO}_2$  group ( $n=12$ ), and  $\text{SO}_2$  group ( $n=6$ ). ISO-induced subacute myocardial injury was produced as described<sup>15</sup> with

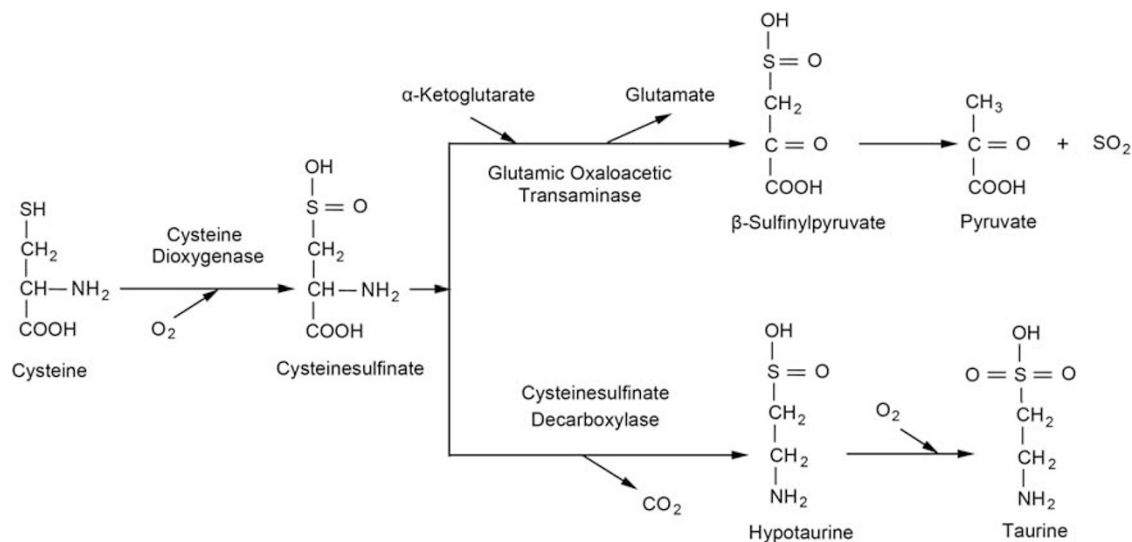


**Figure 1** Sulfur amino acid metabolism pathways. Cysteine oxidase oxidizes cysteine to cysteinesulfinate, and the latter, by decarboxylation and transamination, changes to hypotaurine and sulfinylpyruvate, respectively, and finally metabolizes to taurine and pyruvate, as well as  $\text{SO}_2$ .

minor modifications. Briefly, ISO at a dose of 20 mg/(kg day) was injected (subcutaneously) for 7 days in rats of the ISO-treated group. Rats were injected with 0.9% saline (0.2 ml/day) in the control group. Rats in the ISO + SO<sub>2</sub> group were administered with ISO at a dose of 20 mg/(kg day) (subcutaneously) for 7 days and injected (intraperitoneally) with Na<sub>2</sub>SO<sub>3</sub>/NaHSO<sub>3</sub> (SO<sub>2</sub> donor) at 85 mg/(kg day) for 7 days,<sup>16</sup> whereas rats in SO<sub>2</sub> group were injected only with Na<sub>2</sub>SO<sub>3</sub>/NaHSO<sub>3</sub> at 85 mg/(kg day) for 7 days.

### Echocardiographic Examination

Rats were anesthetized by inhalation of 3% isoflurane and the examination was performed with a 17.5 MHz phased-array Visual Sonics Vevo 770 Imaging System (Toronto, Canada) at the left 30° decubitus position. Two-dimensional parasternal long axis views and short axis views were obtained at the papillary muscle level. Diastolic left ventricular posterior wall thickness (LVPWd) and systolic left ventricular posterior wall thickness (LVPWs) were measured. Ejection fraction (EF) and fractional shortening (FS) were then calculated. All measurements were averaged for three consecutive cardiac cycles and the examination was made by an experienced technician who was blinded to the group identity.

### Determination of Cardiac Function by Cardiac Catheterization

Rats were fasted overnight but had free access to water after the last administration of the drug. At the end of the experiment, rats were anesthetized with 12% urethane (10 ml/kg, intraperitoneally). A catheter filled with heparin saline (500 U/ml) was inserted into the right carotid artery for the development of maximal left-ventricular pressure (LV ± dp/dt max; BL-Newcentury, Chengdu, China). Finally, the rats were killed, the hearts were removed, and the sections were formalin fixed. The rest of the rat hearts were quickly frozen in liquid nitrogen to aid detection of other indicators.

### Myocardial Pathological Examination

Samples of apical ventricular muscle were fixed and dehydrated with 10% formalin. They were then embedded in paraffin and sectioned in increments of 5 μm. They were stained with hematoxylin and eosin (H and E staining) and observed by optical microscopy. Fresh myocardial tissues were cut into pieces (1 mm<sup>3</sup>), fixed with 3% glutaraldehyde, flushed with phosphate-buffered saline (PBS), fixed with 1% perosmic acid, and dehydrated with acetone. Ultrathin sections were placed on 400-mesh grids and double stained with uranyl acetate and lead citrate. Sections were observed under transmission electron microscopy (TEM; JEM1230; Jeol, Tokyo, Japan).

### Stereological Analysis

Five of the ultrathin sections from each rat were selected at random for further stereological analysis in TEM. A total of 10 microscopic fields were randomly chosen at each section

and photographed. Numbers of mitochondrial profiles per picture were counted by the point counting method, as described previously.<sup>17</sup> On the basis of this method, the number of mitochondria per picture (*N*), mean surface area (*S̄*), mean volume (*V̄*), volume density (*V<sub>v</sub>*), surface density (*S<sub>v</sub>*), numerical density (*N<sub>v</sub>*), and specific surface (*R<sub>sv</sub>*, surface-to-volume ratio) of mitochondria were calculated following the B100 double square lattice system with the number of test points *Pt* = 400.<sup>18,19</sup> All of the stereological evaluations were conducted with assistance from a Computerized Hardware–Software System (Motic Med Computer Image Analysis System 6.0; Beijing Motic Image Technology Company, Beijing, China).

### Determination of Tissue Sulfite Content

Sulfite is the hydrated form of SO<sub>2</sub> found in mammalian plasma.<sup>9</sup> We detected the sulfite concentrations in the myocardium tissues to indirectly represent SO<sub>2</sub> content. Sulfite determination was analyzed using HPLC with fluorescence detection (HPLC-FD; LC-20A, Shimadzu, Japan).<sup>20</sup> Briefly, 100 μl of the sample was mixed with 70 μl of 0.212 mol/l sodium borohydride in 0.05 mol/l Tris-HCl (pH 8.5) and incubated at room temperature for 30 min. The sample was mixed with 10 μl of 70 mmol/l mBrB in acetonitrile, incubated for 10 min at 42°C, and mixed with 40 μl of 1.5 mol/l perchloric acid. The protein precipitate in this mixture was removed by centrifugation at 12,400 g for 10 min at 23°C. The supernatant was immediately neutralized by adding 10 μl of 2 mol/l Tris-HCl (pH 3.0) and centrifuged at 12,400 g for 10 min. The neutralized supernatant was used for HPLC. The column (4.6 mm × 150 mm C18 reverse-phase column, Agilent series 1100; Agilent Technologies, Waldbronn, Karlsruhe, Germany) was first equilibrated with a buffer (methanol:acetic acid:water = 5.00:0.25:94.75 by volume; pH 3.4). The sample loaded onto the column was resolved by a gradient of methanol for 0–5 min, 3%; 5–13 min, 3–35%; 13–30 min, 35–62%; 30–31 min, 62–100%; 31–39 min, 100%; 39–40 min, 100–3%; and 40–45 min, 3% at a flow rate of 1.0 ml/min. Sulfite-bimane was measured by excitation at 392 nm and emission at 479 nm. Quantification was carried out by the standardization of Na<sub>2</sub>SO<sub>3</sub>. Sulfite content in tissues was expressed as micromole per gram of protein.

### Assay of GOT Activity

GOT activity in myocardial homogenates was determined by continuous assay and a biochemistry analyzer (Hitachi 7600, Tokyo, Japan). GOT activity in the myocardium was expressed as units per milligram of protein.

### Determination of *GOT1*, *GOT2*, *Superoxide Dismutase 1*, *Superoxide Dismutase 2* and *Glutathione Peroxidase* mRNAs in Tissues

Total RNA in tissues was extracted using Trizol reagent and reverse transcribed by oligo-(dT)<sub>18</sub> primer and MMLV RT.

Primers and probes used are listed in Table 1. Quantitative real-time PCR was carried out on an ABI PRISM 7300 instrument. The PCR mixture contained 5  $\mu$ l of 10  $\times$  PCR buffer, 5  $\mu$ l of cDNA template or standard DNA, 4  $\mu$ l of 2.5 mM per dNTPs, 5 U of Taq DNA polymerase, 1  $\mu$ l of ROX (catalog number 12223-012; Invitrogen, Carlsbad, CA, USA), 15 pmol each of forward and reverse primers, and 10 pmol of TaqMan probe in a total volume of 50  $\mu$ l. Samples and standard DNAs were determined in duplicate. The PCR condition was predenatured at 95°C for 5 min, then 95°C for 15 s, and 60°C for 1 min for 40 cycles. The amount of  $\beta$ -actin cDNA in the sample was used to calibrate the sample amount used for determination.

### Measurement of Oxidants and Antioxidative Enzymes in Myocardium Tissue

Myocardium tissue was rinsed with saline and resected. A ninefold volume of PBS was added, and the mixture was ground gently at 4°C. Concentrations of superoxide

dismutase (SOD) and glutathione peroxidase (GSH-Px) in myocardial homogenates were determined according to the xanthine oxidase method and 5,5'-dithiobis-2-nitrobenzoic acid method provided by standard assay kits (Nanking Jiancheng Biology Company, Nanjing, China), as described previously.<sup>21</sup> Superoxide radical ( $O_2^{\bullet-}$ ) production was assessed from myocardial segments by the lucigenin chemiluminescence (5  $\mu$ mol/l) method, as we previously described.<sup>22-25</sup> Hydrogen peroxide ( $H_2O_2$ ) production in myocardial homogenate was evaluated according to the modified protocols of Miura *et al.*<sup>26</sup>

### Statistics

Results were expressed as mean  $\pm$  s.d. All data were analyzed with SPSS 11.5 (SPSS, Incorporated, Chicago, IL, USA), and analysis of variance (ANOVA) followed by *post-hoc* analysis (Newman-Keuls test) was used to compare differences among groups.  $P < 0.05$  was considered significant.

**Table 1 Primers and TaqMan probes used in quantitative real-time PCR for the measurement of glutamic oxaloacetic transaminase 1, glutamic oxaloacetic transaminase 2, superoxide dismutase 1, superoxide dismutase 2, glutathione peroxidase 1 and  $\beta$ -actin cDNAs in rat**

cDNA	Oligonucleotide	Sequence	Product size (bp)
Glutamic oxaloacetic transaminase 1	Forward primer	5'-CCAGGGAGCTCGGATCGT-3'	79
	Reverse primer	5'-GCCATTGTCTTCACGTTTCCTT-3'	
	TaqMan probe	5'-CCACCACCCTCTCCAACCCTGA-3'	
Glutamic oxaloacetic transaminase 2	Forward primer	5'-GAGGGTCGGAGCCAGCTT-3'	82
	Reverse primer	5'-GTTTCCCCAGGATGTTTGG-3'	
	TaqMan probe	5'-TTTAAGTTCAGCCGAGATGTCTTTC-3'	
Superoxide dismutase 1	Forward primer	5'-AAAGGACGGTGTGGCCAAT-3'	121
	Reverse primer	5'-TCCACCTTGGCCCAAGTCAT-3'	
	TaqMan probe	5'-CTCAGGAGAGCATTCCATCATTGGCC-3'	
Superoxide dismutase 2	Forward primer	5'-CGTCACCGAGGAGAAGTACCA-3'	131
	Reverse primer	5'-GGCTCAGGTTTGTCCAGAAAAT-3'	
	TaqMan probe	5'-AGGCGCTGGCCAAGGGAGAT-3'	
Glutathione peroxidase 1	Forward primer	5'-CGTGCAATCAGTTCGGACAT-3'	131
	Reverse primer	5'-CTCACCATTACCTCGCACTT-3'	
	TaqMan probe	5'-AATGAAGAGATTCTGAATCCCTCAAGT-3'	
$\beta$ -Actin	Forward primer	5'-ACCCGCGAGTACAACCTTCTT-3'	80
	Reverse primer	5'-TATCGTCATCCATGGCGAACT-3'	
	TaqMan probe	5'-CCTCCGTCGCCGGTCCACAC-3'	

TaqMan probe labeled with FAM at the 5'-end and TAMRA at the 3'-end.

## RESULTS

### Parameters of Cardiac Function Evaluated by Echocardiography

LVPWd and LVPWs significantly increased by 30.7 and 21.7% in rats of ISO group compared with those of the control group ( $P < 0.01$ ), whereas they significantly decreased by 14.7 and 9.1% in ISO + SO<sub>2</sub> group compared with those of the ISO group ( $P < 0.05$ ). EF and FS significantly decreased by 23.6 and 32.4% in rats of ISO group compared with those of the control group ( $P < 0.01$ ), whereas they significantly increased by 27.5 and 30.6% in ISO + SO<sub>2</sub> group compared those of the ISO group ( $P < 0.01$ ). The four parameters of cardiac function, LVPWd, LVPWs, EF, and FS, exhibited no variation in SO<sub>2</sub>-treated rats compared with those of controls (all,  $P > 0.05$ ; Table 2).

### Parameters of Cardiac Function Evaluated by Cardiac Catheterization

Compared with control rats, ISO-treated rats showed lowered LV ± dp/dt max values, whose LV + dp/dt max and LV − dp/dt max values decreased by 22.3 and 39.0%, respectively ( $P < 0.01$ ); after administration of exogenous SO<sub>2</sub>, their LV + dp/dt max and LV − dp/dt max values increased by 9.6 and 22.6%, respectively ( $P < 0.01$  and  $P < 0.05$ ). However, there was no significant difference in LV + dp/dt max and LV − dp/dt max values between SO<sub>2</sub>-treated rats and controls (both,  $P > 0.05$ ; Figure 2).

### Myocardial Pathological Changes

H and E staining in the control group showed that cardiomyocytes were arranged in rows, the fiber structure of cardiomyocytes was clear, there was no damage to cardiac fibers, and the cytoplasm was in uniform (Figure 3a). Subcutaneous administration of ISO caused necrosis of myocardial cells, dissolution of cardiomyocytes, and infiltration of monocytes and other inflammatory cells (Figure 3b). After intraperitoneal administration of SO<sub>2</sub>, necrotic foci, proliferation of fiber granulation tissue, and infiltration of

noninflammatory cells were seen (Figure 3c). No damage was observed in myocardial structure by H and E staining in SO<sub>2</sub> group (Figure 3d). Under TEM, samples from rats in the control group showed myocardial fibers that were ordered, and that the sarcoplasmic reticulum (SR) and T tubular structure of mitochondria were clearly observed; the sarcolemma was integrated, and small vascular endothelial cells and the substrate were not damaged (Figure 4a). However, samples from rats in the ISO group showed a focal myocardial fiber structure that was disordered, cardiomyocytes with nuclear condensation, large vacuoles within the cytoplasm, newly-formed vacuoles, and mitochondria that were swollen and whose crests was broken and dissolved. The structure of the rest of the muscle fibers was better. SR and T tubules were in a high degree of expansion, the lamellar body could be seen, and fewer glycogen particles existed; mitochondrial structure and most of the sarcolemma were maintained. Small vascular endothelial cells and substrates showed no obvious abnormalities (Figure 4b). However with treatment of SO<sub>2</sub> donor in ISO + SO<sub>2</sub> group, myocardial fibers were clear, the structure of some mitochondria was clear, but still some mitochondria were mildly swollen. SR and T tubules showed moderate expansion, small amounts of lipid were seen, most of the sarcolemma was integrated, and the structure of small vascular endothelial cells and the substrate were normal (Figure 4c). In rats treated only with SO<sub>2</sub>, the myocardial fibers were normally arranged and the mitochondria were not swollen (Figure 4d).

Stereological analysis of cardiomyocytic mitochondria among the samples from three groups of rats showed a 16% increase in  $\bar{S}$ , 44% in  $\bar{V}$ , and 23% in  $V_v$  of ISO-treated rats when compared with respective control values (all,  $P < 0.01$ ). Mitochondrial N, N<sub>v</sub>, and R<sub>sv</sub> in samples from rats of the ISO-treated group were reduced by 14%, 17%, and 19% (all,  $P < 0.01$ ) when compared with respective control rats. Administration of SO<sub>2</sub> donor, however, markedly attenuated

**Table 2 Echocardiographic parameters in different groups (mean ± s.d.)**

	EF (%)	FS (%)	LVPWs (mm)	LVPWd (mm)
Control (n = 6)	78.2 ± 3.04	48.6 ± 3.00	2.53 ± 0.25	1.66 ± 0.19
ISO group (n = 6)	59.7 ± 3.96 <sup>##</sup>	32.8 ± 2.73 <sup>##</sup>	3.08 ± 0.33 <sup>##</sup>	2.17 ± 0.47 <sup>##</sup>
ISO+SO <sub>2</sub> group (n = 6)	76.2 ± 6.19 <sup>**</sup>	47.3 ± 5.95 <sup>**</sup>	2.80 ± 0.80 <sup>*</sup>	1.85 ± 0.15 <sup>*</sup>
SO <sub>2</sub> group (n = 6)	74.5 ± 2.92	44.8 ± 2.70	2.54 ± 0.30	1.56 ± 0.24

Abbreviations: EF, ejection fraction; FS, fractional shortening; LVPWd, diastolic left ventricular posterior wall thickness; LVPWs, systolic left ventricular posterior wall thickness.

<sup>##</sup> $P < 0.01$  vs control; <sup>\*\*</sup> $P < 0.01$  vs ISO group; and <sup>\*</sup> $P < 0.05$  vs ISO group.

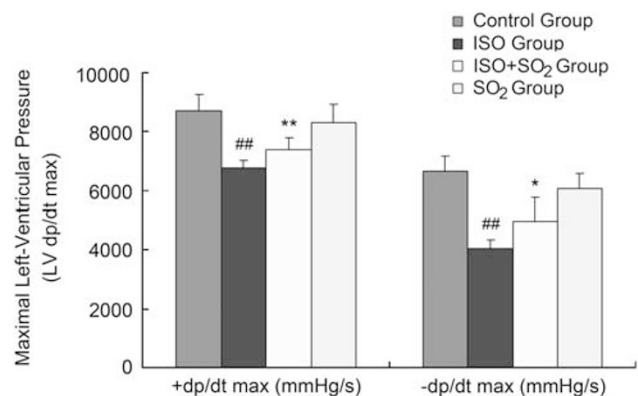


**Figure 2** Maximal left-ventricular pressure (LV ± dp/dt max) in rats of different groups. A catheter filled with heparin saline (500 U/ml) was inserted into the right carotid artery for detecting the development of LV ± dp/dt max. <sup>##</sup> $P < 0.01$  vs control group; <sup>\*\*</sup> $P < 0.01$  vs ISO group; and <sup>\*</sup> $P < 0.05$  vs ISO group.

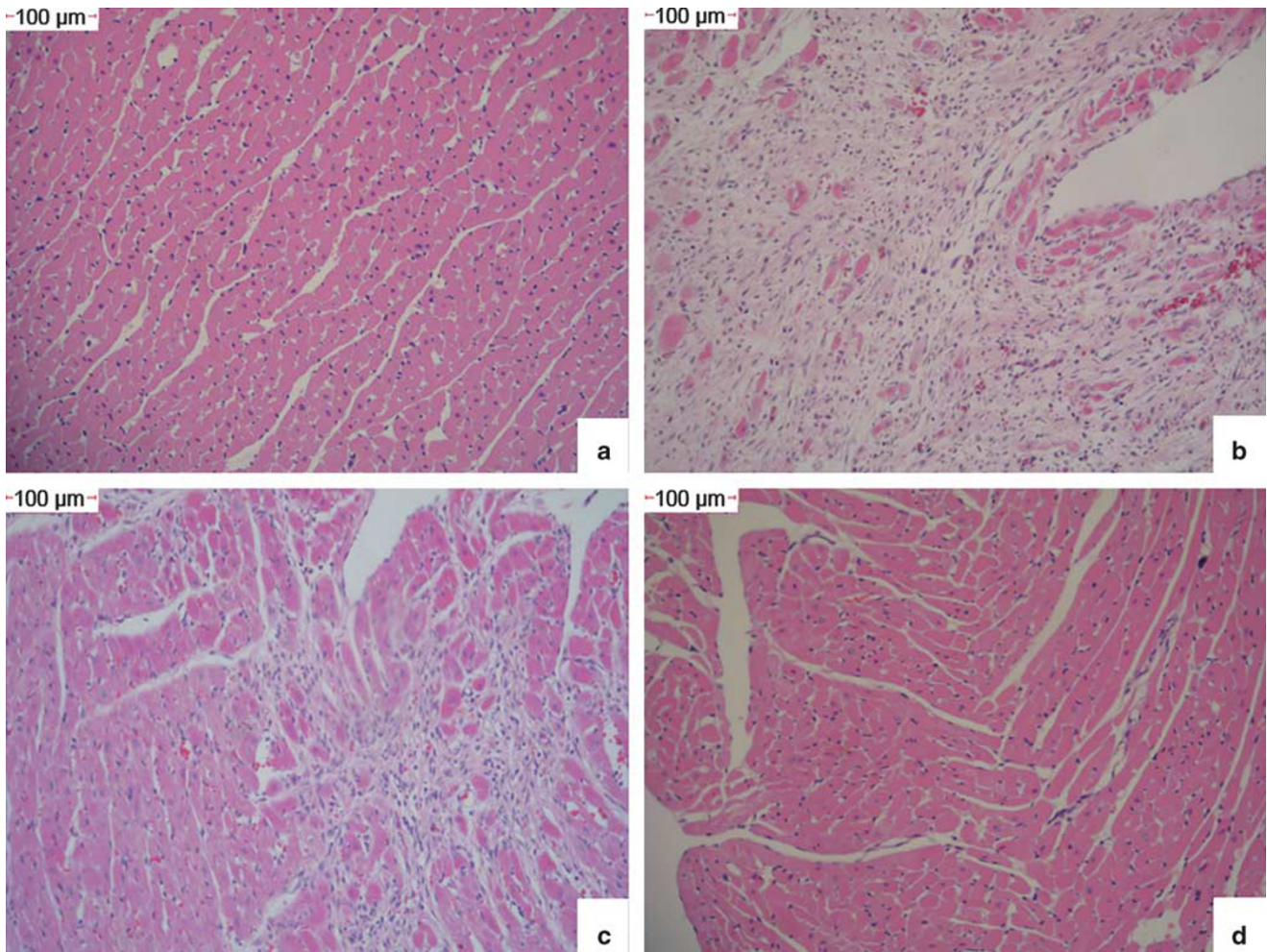


**Figure 3** Microstructural changes in cardiomyocytes. H and E staining in rats showed that in controls (a), the microstructure of cardiomyocytes was normal; in ISO group (b), myocardial structure was damaged. Necrosis of myocardial cells, dissolution of myocardial cells, and infiltration of monocytes and other inflammatory cells were present; whereas in ISO + SO<sub>2</sub> group (c), the damage of myocardial structure was improved; and in SO<sub>2</sub> group (d), the damage of myocardial structure was not observed.

ISO-induced mitochondrial swelling and deformation, as exhibited by a significant reduction in  $\bar{S}$ ,  $\bar{V}$ , and  $V_v$ , and a marked increase in  $N$ ,  $N_v$ , and  $R_{sv}$  of mitochondria ( $\bar{S}$ ,  $\bar{V}$ , and  $V_v$  decreased by 13, 30, and 21%, all,  $P < 0.01$ ;  $N$ ,  $N_v$ , and  $R_{sv}$  increased by 12, 15, and 24%, all,  $P < 0.01$ ) when compared with ISO-treated rats, respectively. There was no significant difference in stereological parameters of cardiomyocytic mitochondria between the controls and SO<sub>2</sub>-treated rats (all,  $P > 0.05$ ; Figure 5).

#### Myocardial Sulfite Level

Sulfite content in the myocardium markedly increased by 61.5% in rats of SO<sub>2</sub> group compared with that of control rats ( $P < 0.05$ ). However, sulfite concentration in rat myocardial homogenates after ISO administration decreased significantly by 41.9% ( $P < 0.01$ ), whereas after administration of a SO<sub>2</sub> donor, sulfite content in the myocardium of

rats increased by 66.0% compared with ISO-treated rats (Figure 6a).

#### Myocardial GOT Activity and *GOT1* and *GOT2* mRNA Expressions

Compared with those of control rats, myocardial GOT activity reduced by 73.9% in ISO-treated rats and by 88.3% in SO<sub>2</sub> group (both,  $P < 0.01$ ; Figure 6b). The *GOT1* mRNA/ $\beta$ -actin mRNA ratio in ISO-treated rat myocardium decreased by 63.4% ( $P < 0.01$ ), whereas the *GOT2* mRNA/ $\beta$ -actin mRNA ratio of myocardium of ISO-treated rats fell by 50.0% ( $P < 0.01$ , Figure 6c). The myocardial *GOT1* mRNA and *GOT2* mRNA did not change in SO<sub>2</sub> group compared with controls (both,  $P > 0.05$ ; Figure 6c). After administration of SO<sub>2</sub>, however, GOT activity, *GOT1* mRNA, and *GOT2* mRNA remained unchanged compared with those of ISO-treated rats (all,  $P > 0.05$ ; Figure 6b and c).

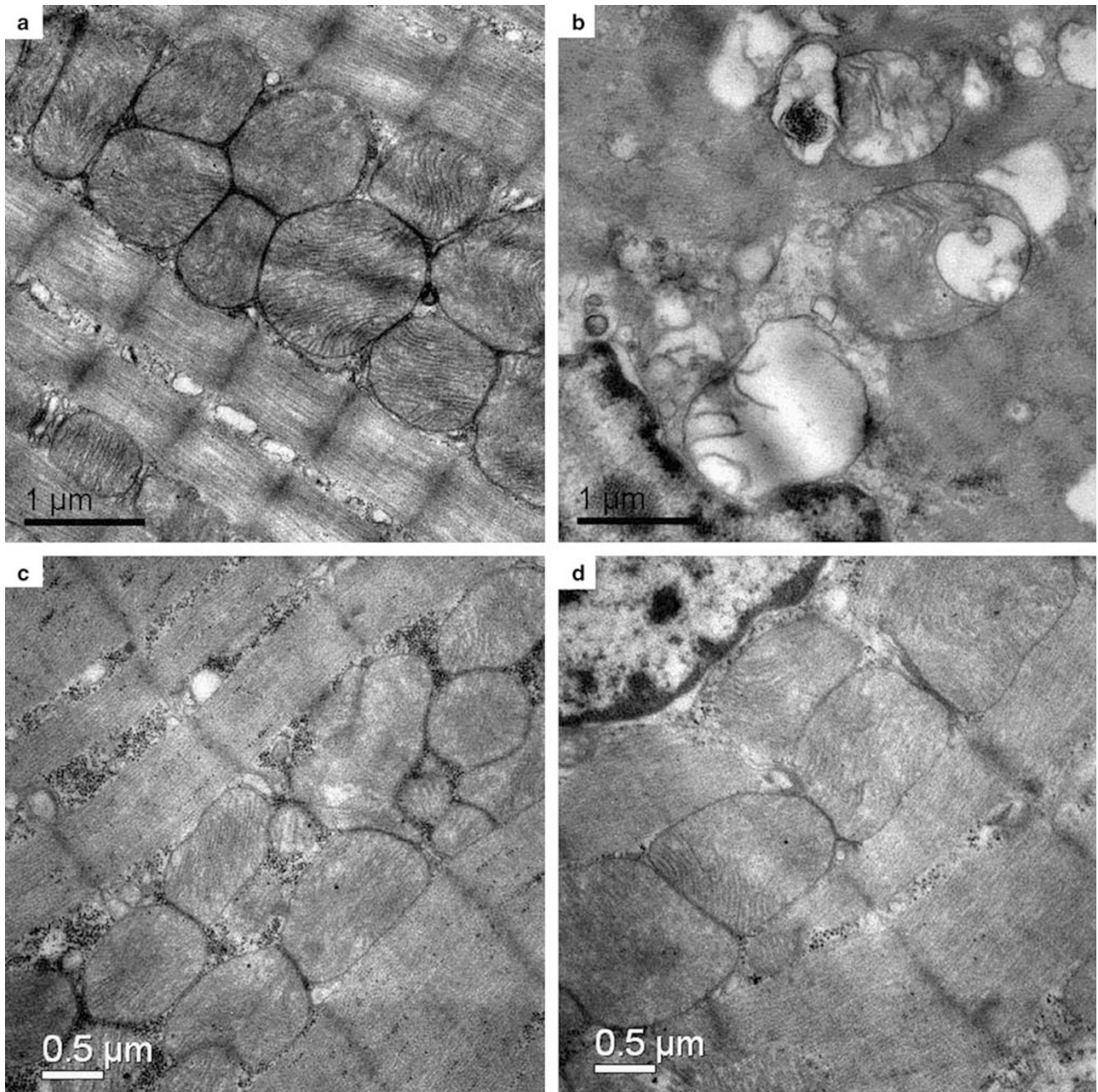


**Figure 4** The ultrastructural changes in cardiomyocytes. Under TEM, it was observed that in rats in control group (a), structure of cardiomyocytes was clearly observed; in ISO group (b), myocardial fiber structure was disordered and mitochondria was swollen; whereas in ISO + SO<sub>2</sub> group (c), part of mitochondria was mildly swollen, and SR and T tubules showed moderate expansion; and in SO<sub>2</sub> group (d), the ultrastructure of cardiomyocytes is similar to the controls.

#### Influence of SO<sub>2</sub> on Oxidative and Antioxidative Balance in ISO-Induced Myocardial Injury

At 7 days after subcutaneous administration of ISO, oxidant production (that is, H<sub>2</sub>O<sub>2</sub> and O<sub>2</sub><sup>•-</sup>) clearly increased ( $P < 0.01$  and  $P < 0.05$ , respectively) compared with those of myocardial homogenates of control rats, but the activity of the antioxidative enzymes SOD and GSH-Px reduced significantly (all,  $P < 0.01$ ), and *SOD1*, *SOD2*, and *GSH-Px1*

mRNAs downregulated by 57.1%, 82.3, and 28.6%, respectively (all,  $P < 0.01$ ; Figure 7). Meanwhile, after the intraperitoneal administration of a SO<sub>2</sub> donor, the activity of SOD and GSH of myocardial homogenates of ISO + SO<sub>2</sub>-treated rats increased by 6.7 and 10.2% ( $P < 0.05$  and  $P < 0.01$ , respectively) and the mRNAs of *SOD2* and *GSH-Px1* in myocardial tissues upregulated by 60.0 and 28.9%, respectively (both,  $P < 0.05$ ), whereas H<sub>2</sub>O<sub>2</sub> and O<sub>2</sub><sup>•-</sup> decreased by

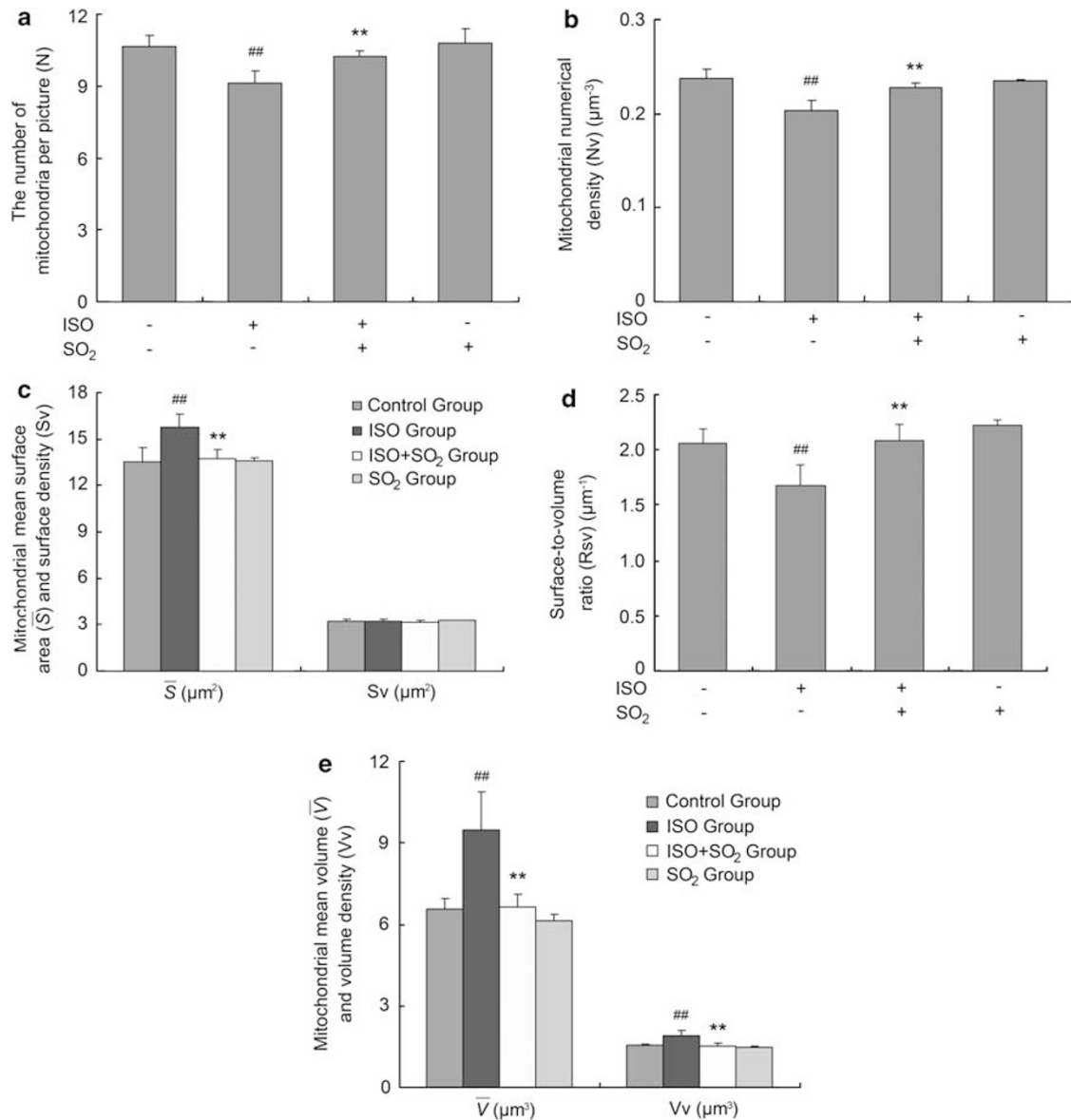


**Figure 5** Stereological analysis of myocardial mitochondria using TEM. A total of 10 microscopic fields were randomly chosen at each section and photographed. **(a)** Mitochondrial number was reduced when rats were treated with ISO compared with controls. However, it was increased in rats of ISO + SO<sub>2</sub> group, as compared with ISO-treated rats. There was no difference between SO<sub>2</sub> group and control group. *N* stands for the number of mitochondria per picture, ISO stands for isoproterenol, and SO<sub>2</sub> stands for sulfur dioxide. **(b)** Mitochondrial numerical density was reduced when rats were treated with ISO, as compared with controls, whereas it was increased in ISO + SO<sub>2</sub> group, as compared with ISO-treated rats. *Nv* of SO<sub>2</sub>-treated group was similar to controls. *Nv* stands for numerical density. **(c)** An increase in average surface area was found in ISO-treated rats compared with that of controls. A significant reduction in mitochondrial  $\bar{S}$  was noted in rats of ISO + SO<sub>2</sub> group compared with ISO-treated rats. The disparities between the control group and SO<sub>2</sub> group were not detected. There was no significant difference in mitochondrial *Sv* among rats of different groups.  $\bar{S}$  stands for average surface area and *Sv* surface density. **(d)** Mitochondrial surface-to-volume ratio was reduced when rats were treated with ISO compared with controls and it was increased in rats of ISO + SO<sub>2</sub> group compared with ISO-treated rats, whereas it showed no changes in SO<sub>2</sub> group compared with controls. *Rsv* stands for surface-to-volume ratio. **(e)** Increases in mitochondrial average volume and volume density were found in ISO-treated rats compared with those of controls; meanwhile, significant reduction in mitochondrial average volume and volume density was noted in rats of ISO + SO<sub>2</sub> group compared with ISO-treated rats, and there was no significant variation between SO<sub>2</sub>-treated and control groups.  $\bar{V}$  stands for average volume and *Vv* for volume density. <sup>##</sup>*P* < 0.01 vs control group; and <sup>\*\*</sup>*P* < 0.01 vs ISO group.

14.7 and 47.6%, respectively, as compared with those of ISO rats (*P* < 0.05; Figure 7). However, mRNA of *SOD1* did not change in rats of the ISO + SO<sub>2</sub> group compared with ISO-treated rats (*P* > 0.05; Figure 7). The content of H<sub>2</sub>O<sub>2</sub> and

O<sub>2</sub><sup>•-</sup> in rat myocardial homogenates showed no statistical variation between control group and SO<sub>2</sub>-treated group (*P* > 0.05), whereas in SO<sub>2</sub>-treated group, the activity of the antioxidative enzymes *SOD1* and *GSH-Px* decreased



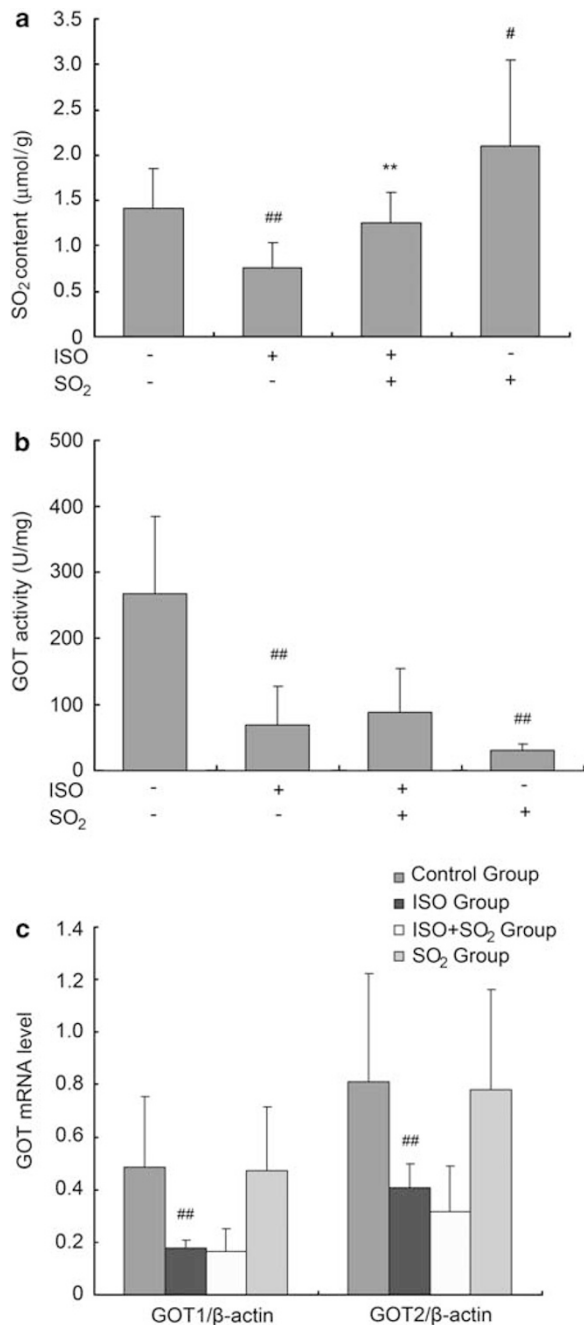


**Figure 6** The changes in sulfur dioxide (SO<sub>2</sub>)/glutamic oxaloacetic transaminase (GOT) pathway in myocardial tissue of isoproterenol (ISO)-induced rats. In ISO-treated rats, myocardial sulfite content decreased compared with the controls, but it increased significantly in rats of ISO + SO<sub>2</sub> group compared with that of ISO-treated rats, and in SO<sub>2</sub> group it was markedly higher than that of controls (a). Myocardial GOT activity reduced in both ISO group and SO<sub>2</sub> group compared with that of control rats, but it did not change in ISO + SO<sub>2</sub> group compared with ISO group (b). GOT1 and GOT2 gene expressions downregulated in ISO-treated rats compared with control rats, but they did not differ between ISO + SO<sub>2</sub> group and ISO group, and between SO<sub>2</sub> group and control group (c). ##*P*<0.01 vs control group; #*P*<0.05, vs control group; and \*\**P*<0.01 vs ISO group.

significantly (*P*<0.01 and *P*<0.05, respectively) accompanied by SOD1 and GSH-Px1 mRNA downregulation (all, *P*<0.01, Figure 7).

## Discussion

Supramaximal doses of the β-adrenergic agonist ISO induced acute myocardial necrosis and interstitial fibrosis.<sup>1,15,27–30</sup> Histopathological lesions produced by ISO in rats resembled those from myocardial infarction in animal models of atherosclerosis.<sup>1</sup> Grimm *et al*<sup>31</sup> showed that supramaximal dosages of ISO led to heart failure, characterized by increases in end-diastolic volume, end-diastolic pressure, left-ventricular wall thickness, and myocardial deposition of fibronectin and laminin. In this study, we used a rat model of ISO-induced myocardial injury to examine the possible role of endogenous SO<sub>2</sub> in the development of myocardial injury.

To examine whether SO<sub>2</sub> donor at a dose of 85 mg/(kg day) impacted the cardiac physiological status of rats, we investigated the cardiac function and structure between normal rats and SO<sub>2</sub>-treated rats. In SO<sub>2</sub> group, the sulfite concentration in myocardial homogenates was markedly higher than that of the controls, whereas the cardiac function and structure remained unchanged, suggesting that the dose of SO<sub>2</sub> donor we used in this study might not influence the cardiac function and structure of normal rats, although it led to a marked increase in SO<sub>2</sub> concentration in myocardium (increased by 61.5%) as compared with controls. The increase in myocardial concentration of SO<sub>2</sub> led to an attenuated myocardial antioxidant capacity demonstrated by the decrease in both mRNA expression and enzyme activity of SOD and GSH-Px. However, the release of free oxygen radicals was not altered. Hence, this impact on myocardial redox status did not reach the extent to which the myocardial injury occurred.

After the treatment of ISO, myocardial contraction and diastolic function were significantly lowered, as demonstrated by decreased +dp/dt max and -dp/dt max, increased LVPWd and LVPWs, and decreased EF and FS. In addition, in ISO-treated rats, H and E staining showed damaged myocardial structure. TEM revealed that the ultrastructures of cardiomyocytes were seriously destructed. The observations stated were typical of myocardial ischemic necrosis. Quantitative analysis of mitochondrial morphology indicated that the myocardial mitochondria of ISO-treated rats became swollen and necrotic. This was correlated with the alterations of mitochondria observed under TEM. The above facts demonstrated that a myocardial ischemic model was created.

Interestingly, in ISO-treated rats, myocardial sulfite content was lower than that of the control group. It has been reported that GOT is a key enzyme in controlling endogenous production of SO<sub>2</sub>.<sup>32,33</sup> Therefore, to investigate why the myocardial content of sulfite decreased in the ISO-treated rats, we examined the GOT activity in myocardium and

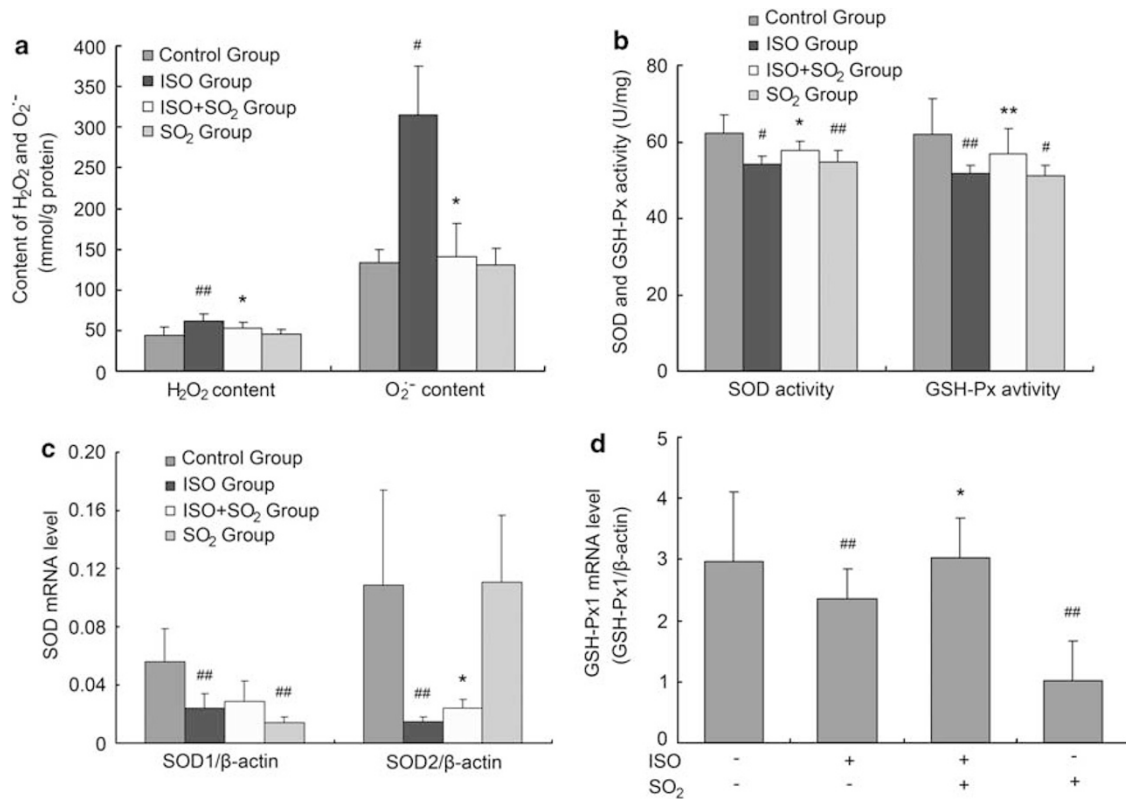


**Figure 7** Measurement of oxidative stress and antioxidative capacities in myocardium tissue. In ISO group, myocardial homogenate H<sub>2</sub>O<sub>2</sub> and O<sub>2</sub><sup>-</sup> increased, compared with those of control rats. Meanwhile, in ISO + SO<sub>2</sub> group, H<sub>2</sub>O<sub>2</sub> and O<sub>2</sub><sup>-</sup> decreased markedly, as compared with those of ISO rats. There was no difference between SO<sub>2</sub>-treated group and the control group (a). The activity of myocardial homogenate SOD and GSH-Px decreased significantly in ISO-treated rats compared with controls, as well as in SO<sub>2</sub> group compared with controls, but they increased in ISO + SO<sub>2</sub> group compared with those of ISO group (b). Both *SOD1* and *SOD2* mRNAs downregulated significantly in ISO-treated rats compared with controls, whereas *SOD2* mRNAs upregulated in ISO + SO<sub>2</sub> group compared with ISO group and *SOD1* mRNAs decreased in SO<sub>2</sub> group compared with controls (c). *GSH-Px1* mRNAs downregulated significantly in both ISO-treated rats and SO<sub>2</sub>-treated rats compared with controls, but upregulated in ISO + SO<sub>2</sub> group compared with that of ISO group (d). <sup>##</sup>*P* < 0.01 vs control group; <sup>#</sup>*P* < 0.05 vs control group; <sup>\*</sup>*P* < 0.01 vs ISO group; and <sup>\*</sup>*P* < 0.05 vs ISO group.

found that it also decreased significantly. Moreover, mRNAs of *GOT1* and *GOT2* were significantly lower than those in the control group. It was indicated that the endogenous SO<sub>2</sub>/GOT pathway was downregulated in myocardial injury induced by ISO.

To explore whether the downregulation of the SO<sub>2</sub>/GOT pathway is involved in the mechanisms responsible for ISO-induced myocardial damage, we treated ISO-injected rats with exogenous SO<sub>2</sub>. By adding exogenous SO<sub>2</sub>, sulfite content of the myocardium was significantly increased, and more interestingly, cardiac function significantly improved. In addition, myocardial pathological changes were obviously alleviated. Stereological analysis of cardiomyocyte mitochondria showed an improvement from the mitochondrial injury. These results are consistent with the alleviation of morphological mitochondrial injury. The data suggest that downregulation of the endogenous SO<sub>2</sub>/GOT pathway probably participated in the mechanisms responsible for myocardial damage induced by ISO.

Until now, the mechanisms by which SO<sub>2</sub> regulates ISO-induced myocardial damage have been unclear. Previous

studies indicated that large doses of ISO induced severe oxidative stress.<sup>1,34</sup> Meszaros *et al*<sup>35</sup> showed that administration of supramaximal dosages of ISO increased end-diastolic volume and end-diastolic pressure, contributing to ventricular dysfunctions, which possibly resulted from the auto-oxidation of catecholamines that stimulated oxidative stress via reactive mediators, leading to cardiotoxicity.<sup>36</sup> More interestingly, the ventricular dysfunction, as mentioned above, could be significantly prevented by antioxidants.<sup>35,37</sup> An increasing body of evidence suggests that free radicals, including reactive oxygen species and reactive nitrogen species, have long been recognized to act as the major mediators of cardiac injury, and antioxidants and free radical scavengers have been shown to minimize cardiac injury, which, to some extent, verifies that oxygen radicals have a key role in cardiac injury.<sup>38,39</sup> Studies showed that ISO-induced cardiotoxicity was partly due to the formation of oxygen-free radicals and sulfhydryl reactivity through a variety of its oxidation products.<sup>2</sup> Cells are protected against oxidative insult by diverse antioxidant enzymes such as SOD and GSH-Px.<sup>40</sup> SOD catalyzes the dismutation of O<sub>2</sub><sup>-</sup> to H<sub>2</sub>O<sub>2</sub> in the extracellular

compartment. The major pathways for the disposal of H<sub>2</sub>O<sub>2</sub> in cells are catalyzed by GSH-Px and catalase, which metabolize H<sub>2</sub>O<sub>2</sub> into water and oxygen. Du and coworkers<sup>41</sup> reported that endogenous SO<sub>2</sub> raised the antioxidant capacity in rats of monocrotaline-induced pulmonary hypertension. In this study, antioxidant activity demonstrated by SOD and GSH-Px in the myocardial tissue of ISO-treated rats decreased significantly. mRNAs of *SOD1*, *SOD2*, and *GSH-Px1* were significantly lower than those of the control group, but O<sub>2</sub><sup>•-</sup> and H<sub>2</sub>O<sub>2</sub> increased significantly compared with control rats. After supplementation with exogenous donors of SO<sub>2</sub>, the activity of SOD and GSH-Px increased, *SOD2* and *GSH-Px1* mRNAs were also upregulated, whereas the content of O<sub>2</sub><sup>•-</sup> and H<sub>2</sub>O<sub>2</sub> decreased, indicating that SO<sub>2</sub> could improve the antioxidant capacity of myocardium and reduce free radicals production. Meanwhile, supplemental SO<sub>2</sub> could ameliorate cardiac function injured by ISO. The results suggested that SO<sub>2</sub> could alleviate myocardial damage induced by ISO via increasing antioxidant capacity. The study also showed that ISO caused a downregulation of endogenous SO<sub>2</sub>/GOT pathway. Taken together, the above findings suggested that the disturbed endogenous SO<sub>2</sub>/GOT pathway is associated with the imbalance of antioxidant/oxidant capacities generated by ISO.

Taken together, these results indicated that the downregulation of the endogenous SO<sub>2</sub>/GOT pathway is probably involved with the pathogenesis of ISO-induced myocardial injury. SO<sub>2</sub> improved ISO-induced myocardial damage and cardiac function in association with increasing myocardial antioxidant capacity.

#### ACKNOWLEDGEMENTS

This work was supported by the National Natural Science Foundation of China (30630031, 30821001 and 30801251), Key Program of Science and Technology, Ministry of Education, China (307001), and the Major Basic Research Program of China (2006CB503807).

#### DISCLOSURE/CONFLICT OF INTEREST

The authors declare no conflict of interest.

- Rona G. Catecholamine cardiotoxicity. *J Mol Cell Cardiol* 1985;17:291–306.
- Singal PK, Yates JC, Beamish RE, *et al*. Influence of reducing agents on adrenochrome-induced changes in the heart. *Arch Pathol Lab Med* 1981;105:664–669.
- Noronha-Dutra AA, Steen-Dutra EM, Woolf N. Epinephrine-induced cytotoxicity of rat plasma. Its effects on isolated cardiac myocytes. *Lab Invest* 1988;59:817–823.
- Rich DQ, Schwartz J, Mittleman MA, *et al*. Association of short term ambient air pollution concentrations and ventricular arrhythmias. *Am J Epidemiol* 2005;161:1123–1132.
- Park SK, O'Neill MS, Vokonas PS, *et al*. Effects of air pollution on heart rate variability: the VA normative aging study. *Environ Health Perspect* 2005;113:304–309.
- D'Ippoliti D, Forastiere F, Ancona C, *et al*. Air pollution and myocardial infarction in Rome: a case-crossover analysis. *Epidemiology* 2003;14:528–535.
- Du SX, Jin HF, Bu DF, *et al*. Endogenously generated sulfur dioxide and its vasorelaxant effect in rats. *Acta Pharmacol Sin* 2008;29:923–930.
- Mitsuhashi H, Ota F, Ikeuchi K, *et al*. Sulfite is generated from PAPS by activated neutrophils. *Tohoku J Exp Med* 2002;198:125–132.
- Ji AJ, Savon SR, Jacobsen DW. Determination of total serum sulfite by HPLC with fluorescence detection. *Clin Chem* 1995;41:897–903.
- Balazy M, Abu-Yousef IA, Harpp DN, *et al*. Identification of carbonyl sulfide and sulfur dioxide in porcine coronary artery by gas chromatography/mass spectrometry, possible relevance to EDHF. *Biochem Biophys Res Commun* 2003;311:728–734.
- Zhang SQ, Du JB, Jin HF, *et al*. Endogenous sulfur dioxide aggravates myocardial injury in isolated rat heart with ischemia and reperfusion. *Transplantation* 2009;87:517–524.
- Beck-Speier I, Dayal N, Maier KL. Pro-inflammatory response of alveolar macrophages induced by sulphite: studies with lucigenin-dependent chemiluminescence. *J Biolumin Chemilumin* 1998;13:91–99.
- Kaye AD, De Witt BJ, Anwar M, *et al*. Analysis of responses of garlic derivatives in the pulmonary vascular bed of the rat. *J Appl Physiol* 2000;89:353–358.
- Meng Z, Geng H, Bai J, *et al*. Blood pressure of rats lowered by sulfur dioxide and its derivatives. *Inhal Toxicol* 2003;15:951–959.
- Rona G, Chappel CI, Balazs T, *et al*. An infarct-like myocardial lesion and other toxic manifestations produced by isoproterenol in the rat. *AMA Arch Pathol* 1959;67:443–455.
- Zhao X, Jin HF, Du SX, *et al*. The effect of sulfur dioxide on blood pressure and aortic structure of spontaneously hypertensive rat. *Chin Pharmacol Bull* 2008;24:327–330.
- Weibel ER. Stereological principles for morphometry in electron microscopic cytology. *Int Rev Cytol* 1969;26:235–302.
- Romek M., Krzysztofowicz E.. Stereological analysis of mitochondria in embryos of *Rana temporaria* and *Bufo bufo* during cleavage. *Folia Histochem Cytobiol* 2005;43:57–63.
- Gong L, Wang ZG, Ran HT, *et al*. Relationship between myocardial ultrasonic integrated backscatter and mitochondria of the myocardium in dogs. *Clin Imaging* 2006;30:402–408.
- Ubuka T, Yuasa S, Ohta J, *et al*. Formation of sulfate from L-cysteine in rat liver mitochondria. *Acta Med Okayama* 1990;44:55–64.
- Mitsuhashi H, Ikeuchi H, Yamashita S, *et al*. Increased levels of serum sulfite in patients with acute pneumonia. *Shock* 2004;21:99–102.
- Yang X, Zhao Y, Zhou Y, *et al*. Component and antioxidant properties of polysaccharide fractions isolated from *Angelica sinensis* (OLIV) DIELS. *Biol Pharm Bull* 2007;30:1884–1890.
- Csiszar A, Ungvari Z, Edwards JG, *et al*. Aging-induced phenotypic changes and oxidative stress impair coronary arteriolar function. *Circ Res* 2002;90:1159–1166.
- Ungvari Z, Csiszar A, Edwards JG, *et al*. Increased superoxide production in coronary arteries in hyperhomocysteinemia: role of tumor necrosis factor- $\alpha$ , NAD(P)H oxidase, and inducible nitric oxide synthase. *Arterioscler Thromb Vasc Biol* 2003;23:418–424.
- Ungvari Z, Csiszar A, Huang A, *et al*. High pressure induces superoxide production in isolated arteries via protein kinase C-dependent activation of NAD(P)H oxidase. *Circulation* 2003;108:1253–1258.
- Miura H, Bosnjak JJ, Ning G, *et al*. Role for hydrogen peroxide in flow-induced dilation of human coronary arterioles. *Circ Res* 2003;92:e31–e40.
- Brilla CG, Maisch B, Rupp H, *et al*. Pharmacological modulation of cardiac fibroblast function. *Herz* 1995;20:127–134.
- Todd GL, Baroldi G, Pieper GM, *et al*. Experimental catecholamine-induced myocardial necrosis I. Morphology, quantification and regional distribution of acute contraction band lesions. *J Mol Cell Cardiol* 1985;17:317–338.
- Jalil JE, Doering CW, Janicki JS, *et al*. Fibrillar collagen and myocardial stiffness in the intact hypertrophied rat left ventricle. *Circ Res* 1989;64:1041–1050.
- Benjamin IJ, Jalil JE, Tan LB, *et al*. Isoproterenol-induced myocardial fibrosis in relation to myocyte necrosis. *Circ Res* 1989;65:657–670.
- Grimm D, Elsner D, Schunkert H, *et al*. Development of heart failure following isoproterenol administration in the rat: role of the renin-angiotensin system. *Cardiovasc Res* 1998;37:91–100.
- Stipanuk MH. Metabolism of sulfur-containing amino acids. *Ann Rev Nutr* 1986;6:179–209.
- Griffith OW. Cysteinesulfinate metabolism, altered partitioning between transamination and decarboxylation following administration of beta-methylene aspartate. *J Biol Chem* 1983;258:1591–1598.

34. Rathore N, John S, Kale M, *et al*. Lipid peroxidation and antioxidant enzymes in isoproterenol induced oxidative stress in rat tissues. *Pharmacol Res* 1998;38:297–303.
35. Meszaros J, Levai G. Ultrastructural and electrophysiological alterations during the development of catecholamine-induced cardiac hypertrophy and failure. *Acta Biol Hung* 1990;41:289–307.
36. Neri M, Cerretani D, Fiaschi AI, *et al*. Correlation between cardiac oxidative stress and myocardial pathology due to acute and chronic norepinephrine administration in rats. *J Cell Mol Med* 2007;11:156–170.
37. Mohanty I, Arya DS, Dinda A, *et al*. Mechanisms of cardioprotective effect of *Withania somnifera* in experimentally induced myocardial infarction. *Basic Clin Pharmacol Toxicol* 2004;94:184–190.
38. Akhlaghi M, Bandy B. Mechanisms of flavonoid protection against myocardial ischemia–reperfusion injury. *J Mol Cell Cardiol* 2009;46:309–317.
39. Kim HJ, Tsoy I, Park JM, *et al*. Anthocyanins from soybean seed coat inhibit the expression of TNF-alpha-induced genes associated with ischemia/reperfusion in endothelial cell by NF-kappaB dependent pathway and reduce rat myocardial damages incurred by ischemia and reperfusion *in vivo*. *FEBS Lett* 2006;580:1391–1397.
40. Iskesen I, Saribulbul O, Cerrahoglu M, *et al*. Trimetazidine reduces oxidative stress in cardiac surgery. *Circ J* 2006;70:1169–1173.
41. Jin HF, Du SX, Zhao X, *et al*. Effects of endogenous sulfur dioxide on monocrotaline-induced pulmonary hypertension in rats. *Acta Pharmacol Sin* 2008;29:1157–1166.